Human Molecular Genetics, 2019, Vol. 28, No. 14 2365–2377

doi: 10.1093/hmg/ddz064
Advance Access Publication Date: 2 April 2019
General Article

GENERAL ARTICLE

Selective serotonin reuptake inhibitors ameliorate MEGF10 myopathy

Madhurima Saha[1], Skylar A. Rizzo[1,2], Manashwi Ramanathan[1], Rylie M. Hightower[3,4], Katherine E. Santostefano[5], Naohiro Terada[5], Richard S. Finkel[6], Jonathan S. Berg[7], Nizar Chahin[8], Christina A. Pacak[9], Richard E. Wagner[2], Matthew S. Alexander[3,4,10,11], Isabelle Draper[12] and Peter B. Kang[1,13,14,*]

[1]Division of Pediatric Neurology, Department of Pediatrics, University of Florida College of Medicine, Gainesville, FL, USA, [2]Medosome Biotec, Alachua, FL, USA, [3]Department of Pediatrics, Division of Pediatric Neurology, Children's of Alabama and the University of Alabama at Birmingham, Birmingham, AL, USA, [4]University of Alabama Birmingham, Center for Exercise Medicine Birmingham, AL, USA, [5]Center for Cellular Reprogramming, Department of Pathology, Immunology and Laboratory Medicine, University of Florida College of Medicine, Gainesville, FL, USA, [6]Division of Pediatric Neurology, Nemours Children's Hospital, Orlando, FL, USA, [7]Department of Genetics, University of North Carolina School of Medicine, Chapel Hill, NC, USA, [8]Department of Neurology, Neuromuscular Division, Oregon Health and Science University, Portland, Oregon, USA, [9]Department of Pediatrics, University of Florida College of Medicine, Gainesville, FL, USA, [10]Department of Genetics, University of Alabama Birmingham, Birmingham, AL, USA, [11]Civitan International Research Center at University of Alabama Birmingham, Birmingham, AL, USA, [12]Department of Medicine, Tufts Medical Center, Molecular Cardiology Research Institute, Boston, MA, USA, [13]Department of Molecular Genetics and Microbiology and Department of Neurology, University of Florida College of Medicine, Gainesville, FL, USA and [14]Genetics Institute and Myology Institute, University of Florida, Gainesville, FL, USA

*To whom correspondence should be addressed at: Division of Pediatric Neurology, Department of Pediatrics, University of Florida College of Medicine. Tel: 3522738921; Fax: 3522948067; Email: pbkang@ufl.edu

Abstract

MEGF10 myopathy is a rare inherited muscle disease that is named after the causative gene, *MEGF10*. The classic phenotype, early onset myopathy, areflexia, respiratory distress and dysphagia, is severe and immediately life-threatening. There are no disease-modifying therapies. We performed a small molecule screen and follow-up studies to seek a novel therapy. A primary *in vitro* drug screen assessed cellular proliferation patterns in Megf10-deficient myoblasts. Secondary evaluations were performed on primary screen hits using myoblasts derived from *Megf10*$^{-/-}$ mice, induced pluripotent stem cell-derived myoblasts from MEGF10 myopathy patients, mutant *Drosophila* that are deficient in the homologue of MEGF10 (Drpr) and *megf10* mutant zebrafish. The screen yielded two promising candidates that are both selective serotonin reuptake inhibitors (SSRIs), sertraline and escitalopram. In depth follow-up analyses demonstrated that sertraline was highly effective in alleviating abnormalities across multiple models of the disease including mouse myoblast, human myoblast,

Received: January 9, 2019. **Revised:** March 18, 2019. **Accepted:** March 21, 2019

Drosophila and zebrafish models. Sertraline also restored deficiencies of Notch1 in disease models. We conclude that SSRIs show promise as potential therapeutic compounds for MEGF10 myopathy, especially sertraline. The mechanism of action may involve the Notch pathway.

Introduction

MEGF10 myopathy, originally described as early onset myopathy, areflexia, respiratory distress and dysphagia (EMARDD) (1), is a congenital myopathy/muscular dystrophy that is caused by mutations in *MEGF10* (2–4), a gene that is expressed in myoblasts and muscle satellite cells (5). The classic EMARDD phenotype has a severe congenital onset with high mortality (1,3). Later onset, milder variants of MEGF10 myopathy have been described (6,7). The EMARDD phenotype bears some phenotypic resemblances to the motor neuron disease spinal muscular atrophy (SMA), especially the subtype spinal muscular atrophy with respiratory distress type 1 (SMARD1); however, the primary pathology in MEGF10 myopathy originates in skeletal muscle rather than the motor neurons.

The MEGF10 protein has an extracellular domain containing 17 EGF-like repeats, a single transmembrane domain and a cytoplasmic domain (8). MEGF10 undergoes tyrosine phosphorylation, which is disrupted with one of the common mutations associated with the disease, C774R (9). The protein also interacts with Notch1 (5,10), a major component of the Notch signaling pathway that is involved in cellular regulation. MEGF10 has homologues across a number of species, including C. elegans (CED-1) (8), *Drosophila* (Drpr) (11,12), zebrafish (megf10) (2) and mice (Megf10) (5,10), with conservation in key domains.

Currently, only supportive treatments are available for MEGF10 myopathy, focusing on respiratory, nutritional and orthopaedic complications. To address this gap in therapy, we conducted a high-throughput screen of a drug compound library, measuring proliferation of Megf10-deficient myoblasts. Among five compounds that yielded significant augmentation of proliferation, two consistently showed the most improvements and were selected as finalists. These two compounds were analyzed further using additional *in vitro* and *in vivo* disease models. A potential mechanism of action involving the Notch pathway was examined. Results from the secondary screens suggest that sertraline shows the greatest promise as a potential therapy for this devastating disease.

Results

Summary of workflow

A summary of the workflow and results, including both the primary screen and secondary evaluations, is presented in Figure 1.

Screening of drug library from the National Institutes of Health Clinical Collection

The entire library was screened via drug treatment and proliferation assays on 96-well plates (Supplementary Material, Fig. S1). Screening of the entire compound library of 725 drugs on *Megf10* shRNA knockdown C2C12 myoblasts in triplicate yielded 14 compounds that showed statistically significant augmentation of cellular proliferation on two separate plates (i.e. a total of six replicates). Those 14 compounds were then tested with dose response experiments, yielding five compounds that consistently yielded augmented myoblast proliferation (Table 2).

In vitro secondary screening of five candidate compounds

Rescue of the proliferation defect displayed by C2C12 cells that overexpress the human disease-causing mutation *MEGF10* C774R (10), as well as by primary myoblasts derived from *Megf10*$^{-/-}$ mice (10) (versus myoblasts from wild-type mice) was observed following treatment with each of the five candidate drugs (Fig. 2A and B, respectively). In addition, treatment of *Megf10* shRNA C2C12 myoblasts with the five candidate drugs was followed by a cell migration assay (Fig. 2C and D). All five drugs yielded improvements for the two assays, with the most impressive recoveries seen for sertraline and escitalopram. A cell adhesion assay yielded similar findings (Fig. 2E).

Clinical vignettes

Family 02 includes a sporadic female proband (02-1) affected by a classic EMARDD phenotype. Subject 02-1 was born after a 39 week gestation via repeat Caesarian section with a birthweight of 6 pounds, 3 ounces, without complications. Hypotonia was noted at 2 weeks. At her last follow-up visit at 5 years, she is able to sit independently when placed and take about five steps with support. She is only able to drink water by mouth; she uses a gastrostomy for all her nutrition and has a tracheostomy with ventilator support at night and sometimes during the daytime. She communicates primarily via a message app on her mobile device but tries to vocalize whenever possible. She has lumbar scoliosis treated by bracing. Neurological examination is notable for bilateral ptosis, diffuse facial weakness, diffuse muscle atrophy, diffuse hypotonia and diffuse severe weakness. She can hold her head up while in a sitting position with some swaying. Reflexes are absent throughout. Electromyography (EMG) showed myopathic features, a muscle biopsy reportedly showed non-specific changes, and whole-exome sequencing identified the mutations in MEGF10 (Table 1).

Family 03 includes a sporadic female proband (03-1) affected by a late onset MEGF10 myopathy phenotype. At the age of 61 years, she developed proximal muscle weakness accompanied by subacute hypercapnic respiratory failure and a requirement for supplemental oxygen. She denied dysphagia, ocular symptoms, fatigability, cramps, muscle fasciculation or sensory symptoms. Prior to onset of symptoms, she was very active, without any significant respiratory or motor symptoms. She had no family history of similar symptoms. Cardiac evaluation (echocardiogram and electrocardiogram) was normal. Pulmonary function tests showed erect forced vital capacity of 17%. Arterial blood gases showed PO_2 77, PCO_2 64 and pH 7.38. A computed tomography scan of the chest with contrast was normal. She had a midline ridge but no cleft palate. Neuromuscular examination showed bilateral scapular winging, pes cavus, lumbar lordosis and protruded abdomen. She had proximal more than distal muscle weakness of the limbs with diffusely absent deep tendon reflexes. Nerve conduction studies, including repetitive nerve stimulation of the left spinal accessory nerve (recording trapezius), left ulnar nerve (recording abductor digiti minimi) and left fibular/peroneal nerve (recording tibialis anterior), were normal.

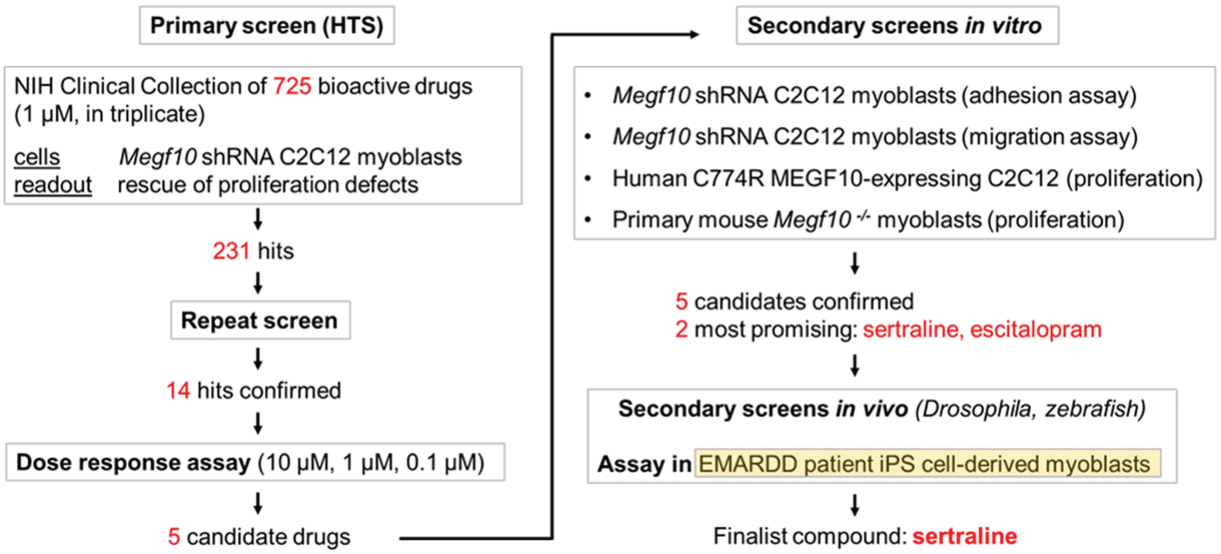

Figure 1. Diagram of workflow illustrating the process of winnowing candidate compounds, from the primary screen to secondary evaluations and determination of the finalist compounds.

Table 1. Summary of three families enrolled with MEGF10 myopathy

Family ID	Phenotype	Mutation 1	Mutation 2
02	EMARDD, early onset, early respiratory failure	c.2320T>C, p.C774R	c.918-2A>G (alters nucleotide in invariant splice acceptor region of intron 8)
27	EMARDD, early onset, late respiratory failure	c.2320T>C, p.C774R	c.976T>C, p.C326R
03	MEGF10 myopathy, adult onset	c.2320T>C, p.C774R	c.3089A>G, p.T1030C

Table 2. Five compounds found to induce increased proliferation on the primary screen of Megf10 shRNA C2C12 myoblasts, with molecular targets in mammalian, zebrafish and *Drosophila* noted

Compound	Mammalian target	Target homolog in zebrafish	Target homolog in *Drosophila*
Sertraline (Sert)	Serotonin transporter, SERT/hSLC6A4	slc6a4a	SerT
Escitalopram (Esci)	Serotonin transporter, SERT/SLC6A4	slc6a4a	SerT
Losartan (Losa)	Type I angiotensin receptor, AGTR1	agtr1	None
Tolterodine (Tolt)	M2/M3 muscarinic receptor	Chrm2/Chrm3	mAcR-60C
Vesamicol (Vesa)	Acetylcholine transporter, VACHT/SLC18A3	slc18a3b	VAChT

Needle electromyography showed fibrillation potentials, positive sharp waves and myotonic discharges with rapidly recruited, short duration, low amplitude complex motor unit potentials in the paraspinal muscles. Single fiber electromyography of the left frontalis, deltoid and extensor digitorum communis was normal. Two prior muscle biopsies from the left thigh and right deltoid showed type 2 fiber atrophy. A third muscle biopsy from the right thigh showed findings suggestive of core-like structures. She had an extensive laboratory work-up, including normal serum creatine kinase and negative acetylcholine receptor binding and modulating antibodies and negative muscle specific kinase antibodies. Biochemical analysis for glycogen storage diseases was negative, and clinical genetic testing for muscular dystrophy, myotonic dystrophy types 1 and 2, ryanodine receptor 1, selenoprotein 1, and facioscapulohumeral muscular dystrophy showed no pathogenic mutations. Mitochondrial electron transport chain analysis and mitochondrial DNA mutation and deletion analysis performed on a muscle biopsy sample was normal. Exome sequencing, performed as part of the NCGENES study (13), identified the presumed causative variants in *MEGF10* (Table 1). At the age of 69 years, she was still ambulatory but had poor exercise tolerance and required BIPAP treatment.

The phenotype for family 027 was previously published, along with mutation analysis (Table 1); this family includes three affected females in a single generation (2).

Myoblast differentiation from human induced pluripotent stem cells

Human peripheral mononuclear blood cells were reprogrammed into induced pluripotent stem cells (iPSCs). Subsequent differentiation of these human iPSCs into myoblasts and myotubes was confirmed via phase contrast microscopy and immunofluorescence (data not shown). Additional confirmation was provided via RT-PCR analyses. Decreased expression of iPSC markers *GATA4*, *NANOG* and *POUF5* was observed in the myoblasts representing both a control subject and a subject with MEGF10 myopathy (27–1), whereas myotubes showed an increase

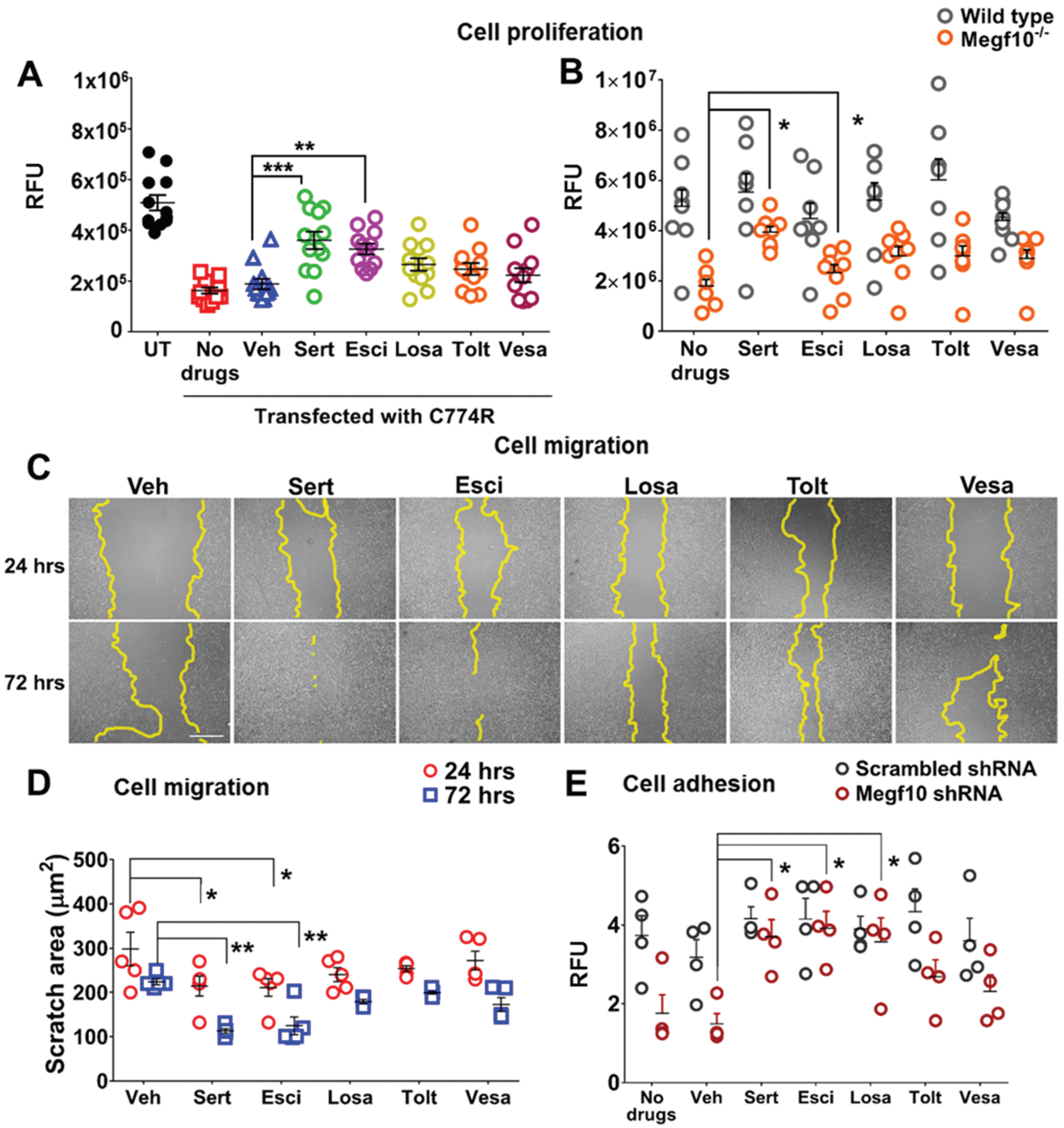

Figure 2. *In vitro* secondary drug screens conducted on C2C12 myoblasts and primary mouse myoblasts. (**A**) Proliferation assay performed with the five candidate compounds on C2C12 cells transfected with V5-tagged C774R mutant Megf10. Drug compounds were administered at 24 h of culture, and CyQUANT assays were performed at 48 h of culture. Statistically significant treatment effects are seen for sertraline (Sert) and escitalopram (Esci). The vehicle was DMSO (Veh). Horizontal bars represent the mean ± S.E.M. from 12 wells in a 96-well plate. On ANOVA, $P < 0.001$. On Bonferroni post hoc t-test, $^{**}P < 0.01$; $^{***}P < 0.001$. (**B**) Proliferation assay performed with the five candidate compounds on primary myoblast cultures from wild type and *Megf10*$^{-/-}$ mice. Drug compounds were administered at 24 h of culture, and CyQUANT assays were performed at 48 h of culture. Statistically significant treatment effects are seen for sertraline and escitalopram. Scatterplots are presented, with horizontal bars representing the mean ± S.E.M. from 8 wells in a 96-well plate. On two-way ANOVA, $P < 0.05$. On Sidak's multiple comparisons test, $^{*}P < 0.05$. (**C**) On migration assay, all five drug candidates yielded improved migration at 24 and 72 h, but the effect was more pronounced for sertraline and escitalopram at 72 h. Irregular yellow lines show borders between cellular and acellular zones for each image. Scale bar, 5 mm. (**D**) Quantifications of residual clear areas on the migration assay using ImageJ software at indicated time points. On two-way ANOVA, $P < 0.05$. On Sidak's multiple comparisons test $^{*}P < 0.05$; $^{**}P < 0.01$; n = 5 images. (**E**) An adhesion assay was performed on Megf10-deficient myoblasts and scrambled shRNA control myoblasts using the five candidate compounds. Megf10 shRNA-treated cells recovered significantly with Sert, Esci and Losa compounds at 60 min time points. Horizontal bars represent the mean fluorescence intensities of the adherent cells ± S.E.M. from two independent experiments, n = 2 per experiment. On two-way ANOVA, $P < 0.05$. On Sidak's multiple comparisons test, $^{*}P < 0.05$.

in the expression of *DES* (Supplementary Material, Fig. S2A). Myoblasts representing subjects with MEGF10 myopathy (03-1, 27-1, 27-2, 27-3, 02-1) showed diminished expression of *MEGF10* and *NOTCH1* compared to myoblasts representing a healthy control subject (H) (Supplementary Material, Fig. S2B).

Functional assays on myoblasts derived from human iPSCs

CyQUANT assay on iPSC-derived human myoblasts from three MEGF10-deficient subjects (proband 02-1, 03-1 and 27-1) shows impaired proliferation versus that seen with myoblasts derived

from healthy subjects (Fig. 3A). Treatment with sertraline hydrochloride leads to significant improvement of proliferation in all affected cell lines (Fig. 3B). A scratch test shows that MEGF10-deficient myoblasts also display impaired migration compared to that seen in healthy control, and carrier parents, myoblasts. Sertraline hydrochloride-treated diseased myoblasts show improved migration at both 72 h and 120 h timepoints (Fig. 3C, with quantifications in Figs 3D and E). RT-PCR reveals significantly reduced expression of *MEGF10, NOTCH1, PAX7, ITGA7* and *MYOD* in myoblasts representing a subject with MEGF10 myopathy (02-1) compared to myoblasts representing an asymptomatic carrier subject (02-3) (Fig. 3F).

Notch pathway analysis of myoblasts

Sertraline hydrochloride was administered to Megf10 shRNA knockdown C2C12 myoblasts and wild-type cells. Protein was extracted from the cells at 24, 48 and 72 h timepoints after dosing. Untreated (vehicle alone) shRNA cells show a deficiency in Notch1 level (versus normal levels in wild type cells). Sertraline treatment of shRNA cells results in a marked increase in the levels of Notch1 that peaks at 24 h and attenuates afterwards (Fig. 3G).

Effects of Notch pathway inhibition and serotonin activation on sertraline treatment in murine and human myoblasts

DAPT attenuated the therapeutic effects of sertraline hydrochloride in Megf10 deficient C2C12 myoblasts (Fig. 4A) and human MEGF10-deficient myoblasts (02-1, 03-1, 27-1) (Fig. 4B). A dose response study on these human MEGF10-deficient myoblast lines showed that DAPT's inhibitory effect on sertraline therapy was present at 5 μM and became more pronounced at 10 μM (Supplementary Material, Fig. S3). Serotonin did not have a significant effect on sertraline treatment.

The effects of sertraline treatment on various components of the Notch pathway in human MEGF10-deficient myoblasts

On RT-PCR analysis, 15 of 43 Notch signaling genes were upregulated in all three human MEGF10-deficient myoblast lines with sertraline hydrochloride treatment compared to untreated healthy controls (Fig. 4C) and untreated MEGF10-deficient myoblasts (Fig. 4D). Among these 15, *NOTCH, MAML* and *JAG* showed the most prominent and consistent changes (Fig. 4E).

Drosophila mutant in vivo screens

We previously demonstrated that $drpr^{\Delta 5}$ mutant *Drosophila* (that lack Drpr, the fly homolog of mammalian MEGF10) display a shortened lifespan, decreased locomotor activity and abnormal muscle histology (11). Under the conditions of the drug screen (detailed in Methods), a decrease in the lifespan of $drpr^{\Delta 5}$ null flies versus that of heterozygous $drpr^{\Delta 5}$ siblings can be seen over the course of several days. This parameter was used as a readout to assess drug efficacy. A preliminary study of both sertraline and citalopram showed rescue effects for both drugs when measuring lifespans (Supplementary Material, Fig. S4). The flies feed directly on the drug (or vehicle alone), which is delivered on horizontally positioned Q-tips (Fig. 5A) saturated with the solution. Sertraline treatment leads to partial rescue of the lifespan of $drpr^{\Delta 5}$ null flies. The effect of the drug is seen in both females (Fig. 5B) and males (Fig. 5C) bearing the $drpr^{\Delta 5}$ deletion in one genetic background; similar results are seen in females (Fig. 5D) and males (Fig. 5E) bearing the $drpr^{\Delta 5}$ deletion in a different genetic background. Gender-specific differences are observed; of note, differential sensitivity of male and female *Drosophila* to drug treatment has been documented previously (14,15). In contrast to sertraline, treatment with the biogenic amine serotonin (5-HT, the ligand of the reuptake transporter that is blocked by sertraline) does not rescue the shortened lifespan of the null mutant flies (Fig. 5F).

Mutant megf10 zebrafish

Antisense morpholino (MO) knockdown of *megf10* in zebrafish yields muscle morphological and motor abnormalities (2); however, a germline mutant line would establish a more uniform model. We established a colony of mutant *megf10* zebrafish (allele sa13029 at the Zebrafish Mutation Project of the Wellcome Trust Sanger Institute) that contains a T>A nonsense mutation (exon 5, amino acid 110). The *megf10* homozygous mutant zebrafish are viable, but showed a slight delay in somite formation that was eventually restored after 3 dpf. The *megf10* mutant fish show muscle defects on phase contrast microscopy and birefringence (Fig. 6A–D) at 4 dpf that phenocopy MO knockdown fish described previously by our group (2). We then demonstrated that pharmacologically relevant doses (0.1 and 1 μM) of sertraline and escitalopram ameliorated megf10-associated muscle pathologies with respect to the *megf10* mutant tail bending phenotypes and survival curves when directly compared to vehicle-treated control *megf10* mutant fish (Fig. 6E–H). These studies demonstrate that the selective serotonin reuptake inhibitor (SSRI) compounds sertraline and escitalopram rescue megf10-dependent pathologies in a vertebrate model of MEGF10 myopathy. Further testing is warranted in rodent models of MEGF10 myopathy to determine the long-term effects and ameliorative capacity of sertraline and escitalopram in other tissue types and stages of MEGF10 myopathy disease progression.

Discussion

Our findings indicate that sertraline, an SSRI, ameliorates the phenotype of MEGF10 myopathy in every disease model studied, including myoblasts (mouse-derived and human-derived), *Drosophila* and zebrafish, revealing its potential as a novel therapy for MEGF10 myopathy. In addition to highlighting the utility of integrating disease models in a translational pipeline, the present study yields insights into the interactions between the Notch pathway and muscle development. Together, our data help define a roadmap to identify novel therapies for ultra-rare diseases and to begin probing novel mechanisms of action for repurposed drugs.

There is accumulating evidence that SSRIs have therapeutic potential in various muscle diseases. Fluoxetine, another SSRI, has been suggested as a therapeutic candidate for complications of myotonic dystrophy type 1 based on a small patient series (16) and for the therapy of Duchenne muscular dystrophy based on zebrafish studies (17), but corresponding new indications have not been approved by the US Food and Drug Administration. Fluoxetine has also been documented to be distributed in human skeletal muscle after standard dosing, albeit at lower levels than in brain, suggesting that oral dosing should be feasible but that higher doses may need to be explored to determine potential efficacy in skeletal muscle (18).

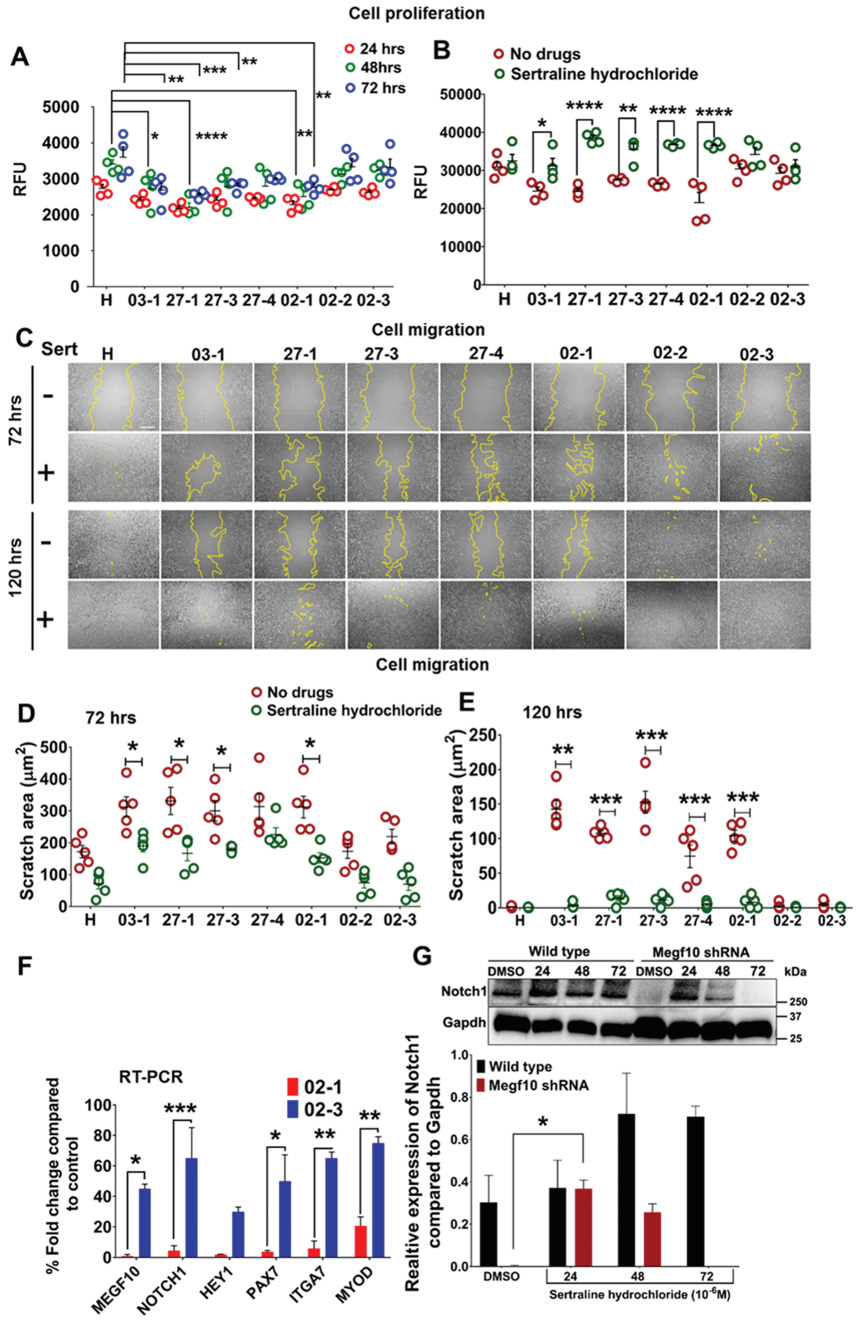

Figure 3. Analysis of sertraline treatment in human iPSC-derived MEGF10-deficient myoblasts and murine Megf10-deficient myoblasts. (**A**) iPSC-derived human myoblasts representing MEGF10 deficiency (02-1, 03-1, 27-1 27-3, 27-4) showed impaired proliferation compared to asymptomatic carrier parents (02-2, 02-3) and a healthy control (H) at 48 and 72 h time points. A two-way ANOVA showed $P < 0.0001$. Bonferroni post test results are indicated on the graph: $^{*}P < 0.05$; $^{**}P < 0.01$; $^{***}P < 0.001$; $^{****}P < 0.0001$. (**B**) Human MEGF10-deficient myoblasts showed significantly improved proliferation compared to untreated myoblasts at 72 h after 1 μM sertraline hydrochloride treatment. Two-way ANOVA showed $P < 0.0001$. Bonferroni post-test results are depicted on the graph: $^{*}P < 0.05$; $^{**}P < 0.01$; $^{****}P < 0.0001$. (**C**) A migration assay performed on iPSC-derived human myoblasts demonstrated marked impairment in migration for MEGF10-deficient myoblasts compared to carriers and a healthy control. The yellow lines mark the borders between cellular and acellular zones. Sertraline treatment induced a marked improvement in migration patterns compared to untreated controls at 72 and 120 h. Scale bar, 5mm; +, sertraline treatment; −, no drug treatment. (**D,E**) Quantification of clear areas on migration assay using ImageJ software at indicated time points. On two-way ANOVA, $P < 0.05$. Sidak's multiple comparisons test $^{*}P < 0.05$, $^{**}P < 0.01$. (**F**) Expression levels of MEGF10, NOTCH1, HEY1, PAX7, ITGA7 and MYOD are compared via RT-PCR in MEGF10-deficient iPSC-derived myoblasts (02-1) versus carrier parent myoblasts (02-3). Data represent mean ± SEM relative to controls performed in triplicate and are presented as percentages of control myoblast expression levels. On two-way ANOVA, $P < 0.05$. Sidak's multiple comparisons test results are indicated on the graph; $^{*}P < 0.05$, $^{**}P < 0.01$; $^{***}P < 0.001$. (**G**) Notch1 protein expression is increased in Megf10 shRNA knockdown and wild-type C2C12 myoblasts after sertraline hydrochloride treatment, most notably at 24 and 48 h. Notch1 augmentation attenuates in the Megf10 shRNA myoblasts by 72 h. Gapdh was used as a loading control. Immunoblot images (top) and their quantification by ImageJ (bottom) are shown. The ImageJ graphs represent data from four independent experiments. Two-way ANOVA shows $P < 0.001$. Tukey's multiple comparison post-test results are depicted on the graph; $^{*}P < 0.05$.

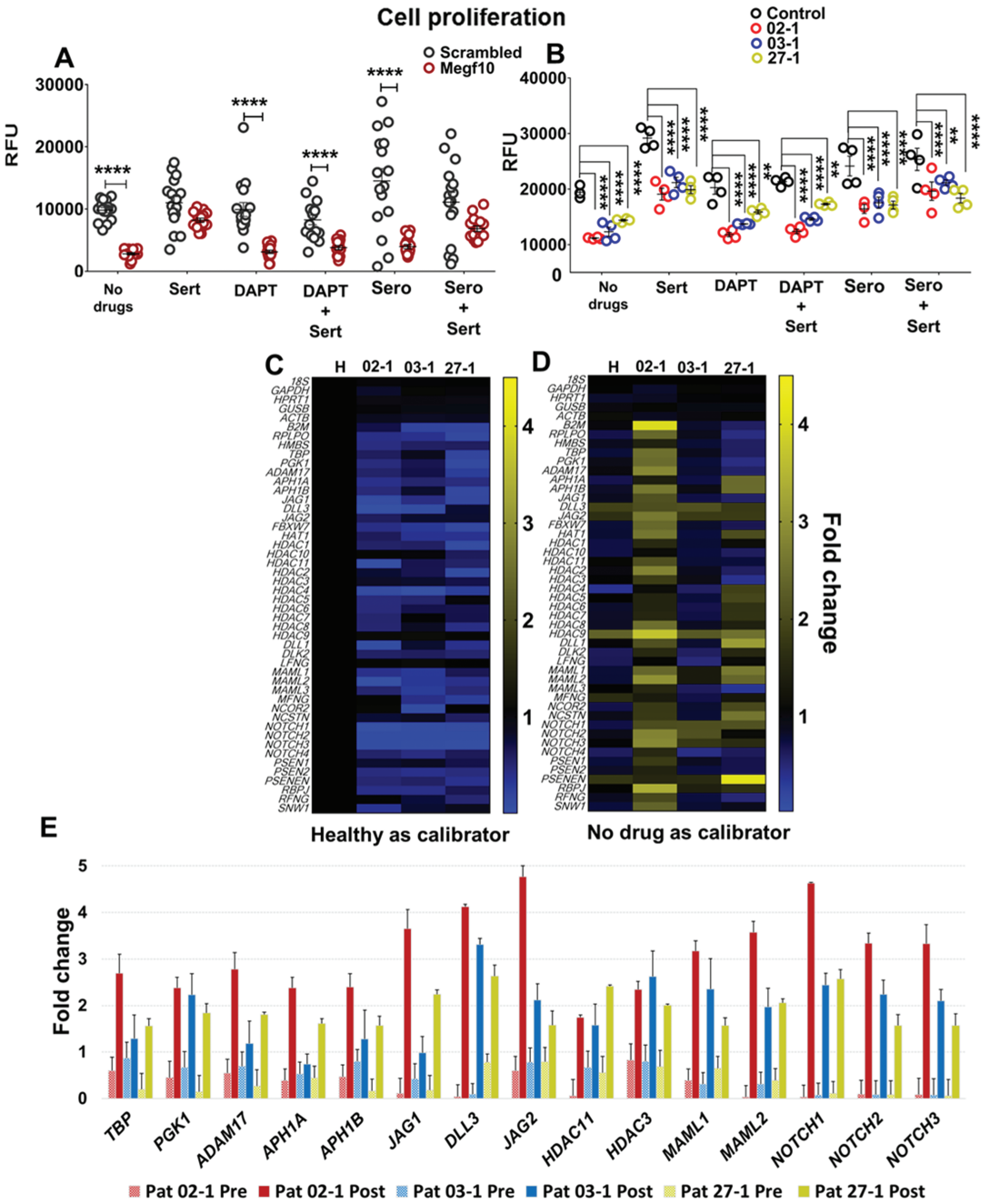

Figure 4. Sertraline treatment reactivates the Notch pathway in murine Megf10-deficient myoblasts and human MEGF10-deficient myoblasts. (**A**) Cell proliferation assays were performed on Megf10-deficient and wild type C2C12 myoblasts that were treated with sertraline alone, sertraline with DAPT and sertraline with serotonin. Three individual experiments with 16 wells are shown. A two-way ANOVA test was performed on different groups and conditions with Sidak's post test, scatter plots representing the mean absorbance ± S.E.M. (****$P < .0001$). (**B**) Cell proliferation assays were performed on MEGF10-deficient human myoblasts (02-1, 03-1, 27-1) and healthy control myoblasts (H). The scatter plots indicate two independent experiments. A two-way ANOVA test was performed on different groups and conditions with Sidak's post test, scatter plots representing the mean absorbance ± S.E.M. (**C**) The heat map represents mRNA expression levels measured via RT-PCR of human Notch signaling genes in human MEGF10-deficient myoblasts treated with sertraline compared to untreated healthy control myoblasts. Genes are located horizontally and samples vertically in the order given. Each sample is represented by the mean of the gene expression value of the samples within that subgroup. Healthy control is the calibrator. Blue indicates down regulation. (**D**) The heat map represents mRNA expression levels measured via RT-PCR of human Notch signaling genes in human MEGF10-deficient myoblasts treated with sertraline compared to untreated healthy control myoblasts. No drug treatment is the calibrator. Yellow indicates relative upregulation, and blue indicates relative downregulation. (**E**) Significant fold changes for the indicated genes were plotted as the mean fold change relative to the expression of the same genes in healthy untreated control subjects. Multiple unpaired *t*-tests were performed and $P < 0.05$ was considered significant.

The Notch pathway in general, and Notch1 in particular, is a key regulator of satellite cell and myoblast physiology (19). Notch1 interacts with both MEGF10 (5,10) and the serotonin pathway (20–22). SSRIs primarily influence serotonin signaling, but they also have an impact on the Notch pathway (21–24). Our current data suggest that SSRIs have the potential to ameliorate

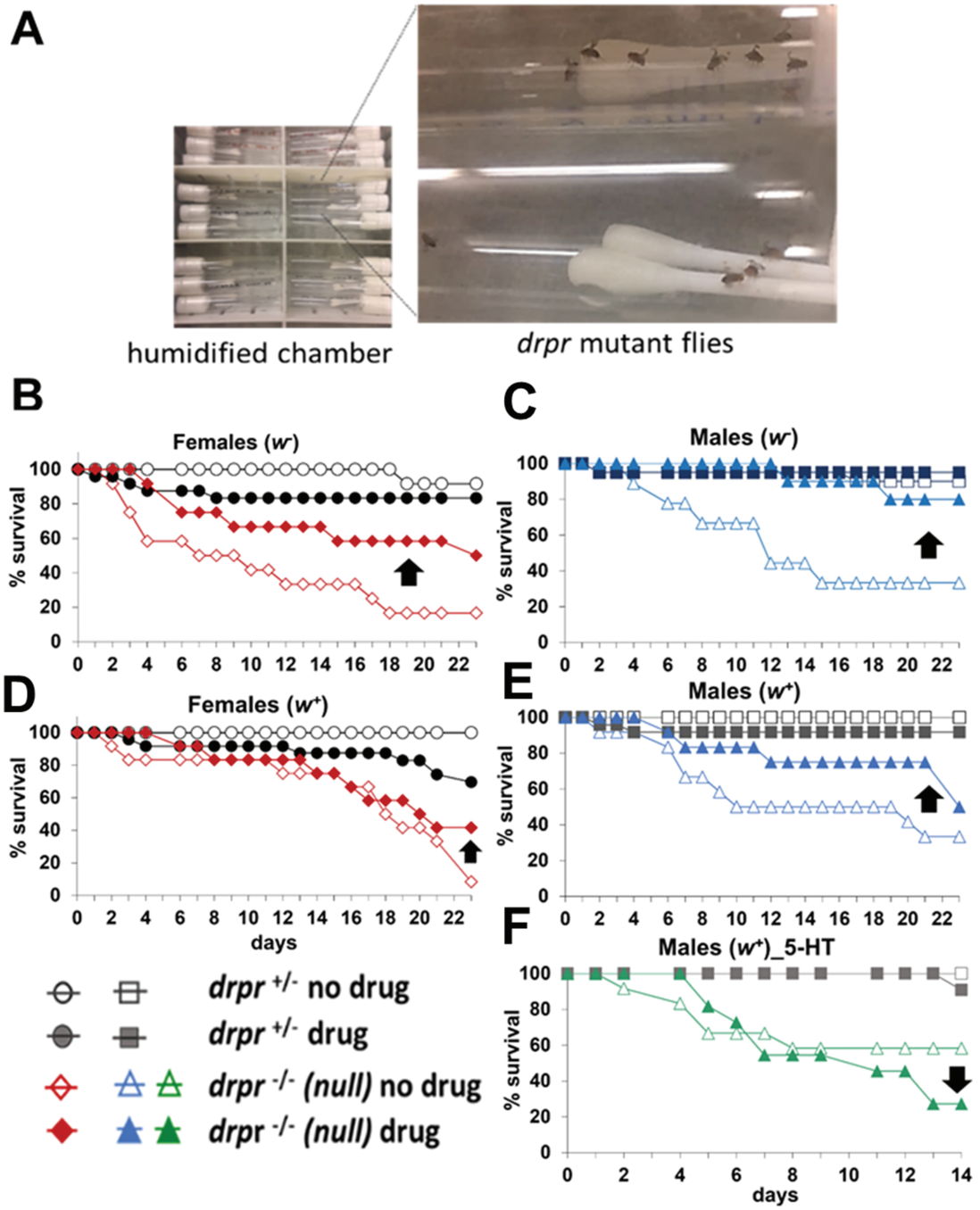

Figure 5. Sertraline treatment of *drpr*-deficient flies. Groups of one day-old $drpr^{\Delta 5}$ heterozygous (*drpr* $^{+/-}$) and null (*drpr* $^{-/-}$) sibling flies were isolated and treated daily with a 10^{-4} M solution of the drug (in 0.1% DMSO, 10% sucrose) or with no drug (0.1% DMSO, 10% sucrose). (**A**) Photographs of the drug delivery system show $drpr^{\Delta 5}$ adult mutant flies being exposed to Q-tips saturated with the various drugs, in vials that are placed horizontally in a humidified chamber. (**B–E**) Sertraline treatment yields partial rescue (straight arrow) of the shortened lifespan displayed by female and male *drpr* null flies over the course of several days. Of note, flies bearing the $drpr^{\Delta 5}$ mutation in two different genetic backgrounds were examined separately: background 1 is the original *white*$^{-}$ (w^{-}) isogenic background and background 2 is the wild-type w^{+} background, in which the *drpr* mutation was backcrossed. (**F**) Treatment of *drpr* null *Drosophila* with the biogenic amine serotonin (5-HT, the ligand of the reuptake transporter that is blocked by sertraline) does not improve survival. n = 9–14 flies per genotype; F, females; M, males.

some of the features of MEGF10 myopathy, acting in part via the Notch pathway. It is notable that sertraline shows effect in *drpr*-deficient flies, suggesting that the drug triggers compensatory processes downstream of DRPR (or in pathways that intersect) to mediate phenotypic rescue. In particular, augmentation of Notch1 activity may play a role in the effects seen in our disease models. Sertraline (25) and escitalopram (26) have been shown to inhibit voltage-dependent K+ channel activity in smooth muscle cells, suggesting another potential mechanism to be investigated in a future study. It is notable that serotonin treatment did not rescue the *drpr*-deficient flies, suggesting that the mechanism of action of sertraline in this context is independent of effects

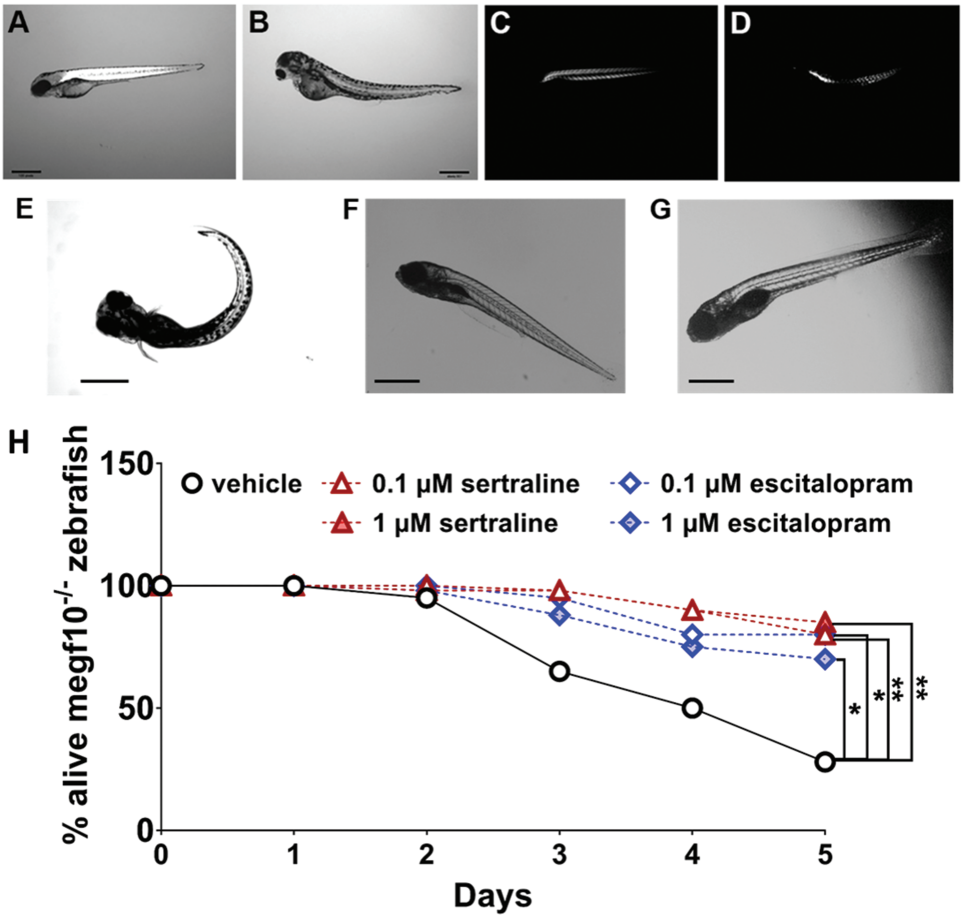

Figure 6. Megf10-deficient zebrafish. Using brightfield microscopy, (**A**) the wild-type zebrafish maintains a straight posture, while (**B**) the megf10 mutant displays significant tail bending (a manifestation of severe dorsal muscle weakness). Birefringence microscopy, (**C**) the wild type zebrafish refracts polarized light off its dorsal muscles, whereas (**D**) the *megf10*-deficient zebrafish has black patches indicating muscle wasting, disorganized muscle fibers and myofiber degeneration pathology. Zebrafish are photographed at 4 dpf. Scale bar, 500μm. Preliminary treatment studies of sertraline and escitalopram in megf10-deficient zebrafish. Each drug cohort included 25 fish from heterozygous matings, and all fish were analyzed at 5 dpf. (**E**) Vehicle treated fish showed significant tail bending pathologies that were prevented with (**F**) 1 μM sertraline and with (**G**) 1 μM escitalopram. (**H**) Survival curves show markedly improved survival for all treatment groups. Percent of living fish were determined by detecting heartbeats. Data represent mean ± SEM relative to controls. On two-way ANOVA, $P < 0.05$. Sidak's multiple comparisons test results are indicated on the graph; $^{*}P < 0.05$, $^{**}P < 0.01$. Scale bar, 1 mm.

on serotonin activity. Furthermore, the *Drosophila* model used in the current experiments was generated by a null mutation that does not express Drpr at all and would be expected to be resistant to Drpr upregulation mechanisms. These lines of evidence suggest that the mechanism of action of sertraline runs parallel to or downstream of direct actions of MEGF10 itself, perhaps incorporating the Notch pathway, without contributions from manipulations of serotonin activity. Thus, further investigation of the use of SSRIs in a mammalian model of MEGF10 myopathy may yield not only knowledge relevant to a novel therapy for this disease but also a deeper understanding of the interactions of MEGF10 and Notch1 during the process of myogenesis.

To push the development of sertraline for the treatment of MEGF10 myopathy further down the drug development pipeline, preclinical mammalian studies will be needed. As both sertraline and escitalopram are already approved by the US Food and Drug Administration for the treatment of depression, it is tempting to initiate human clinical trials immediately. Sertraline is also approved for children aged 6 years and older for the treatment of obsessive–compulsive disorder, but is not routinely used in infants and young children, an age range relevant to MEGF10 myopathy. Potential side effects with early administration of SSRIs have been suggested in rodent (27,28) and human (29) studies, thus the behavior of sertraline in a juvenile mammalian model may be warranted prior to the initiation of human clinical trials. Unexpected side effects occasionally arise when an approved drug is studied in a new patient population, as occurred when a trial of pentoxifylline in Duchenne muscular dystrophy was associated with intolerable gastrointestinal side effects in study participants (30,31). As a *Megf10*$^{-/-}$ mouse has been generated (32) and characterized (10) with respect to a muscle phenotype, it would make sense to use this mouse for such efficacy, pharmacokinetic and safety studies.

The general approach presented here, of using a range of *in vitro* and non-mammalian *in vivo* models of a rare disease to screen drugs for potential novel therapies, can be applied to a broad range of inherited neuromuscular diseases, as well as rare diseases in general. iPSCs derived from human tissue samples (33,34) serve as valuable models of human disease (35,36), especially when differentiated into relevant cell lines (37,38). Zebrafish are powerful tools for identifying and testing novel therapeutic compounds for the treatment of neuromus-

cular diseases due to their abilities to rapidly uptake small molecule compounds through their skin and gills during their larval stages of development (39). *Drosophila* also offer multiple advantages in translational studies. Fruit flies can be maintained at low cost, have homologs to many human disease genes and are highly amenable to medium throughput screens. *Drosophila* models have been successfully used in drug discovery platforms (40,41). Notably, the list of rare human neuromuscular disorders that are modeled in flies is rapidly expanding (42). It is thus tempting to use these new models in established pipelines that integrate target-based as well as phenotypic-based screens (*in vitro* and *in vivo*). Consistent drug effectiveness across multiple disease models may expedite the identification of more promising therapeutics, which may then be tested in mammalian models such as mice prior to human clinical trials.

Materials and Methods

Immortalized myoblast models generated by Megf10 shRNA knockdown

C2C12 myoblasts (American Type Culture Collection) were cultured in Dulbecco's modified Eagle's medium (DMEM, Corning) with 20% fetal bovine serum (Sigma), penicillin (50 units/mL) and streptomycin (50 µg/mL; Invitrogen). A cocktail of three Megf10 short hairpin RNAs (shRNAs), TGTTGGTGCAAGTACAAAC, TCATAGACATTCCTGTTGG, ATTCTCTGGCAAGTGGTGC, was transfected into C2C12 cells that had been plated in medium without antibiotics inserted into a pZIP vector containing green fluorescent protein (GFP) (GE Healthcare Dharmacon) was transfected into C2C12 cells that had been plated in medium without antibiotics. Scrambled shRNA was transfected into separate cultures as a control. GFP expression was monitored for 48 h after transfection to determine transgene expression. Selected Megf10 and scrambled shRNA colonies displaying GFP expression were grown in media containing puromycin (4 µg/mL) according to a puromycin death curve generated for C2C12 myoblasts (10).

Primary drug screen using Megf10 shRNA knockdown myoblasts

The compound library consisted of 725 bioactive drugs from the National Institutes of Health Clinical Collection that were made available via Evotec, A.G. (Hamburg, Germany). These compounds are either already approved by the US Food and Drug Administration or have been studied in phase I–III clinical trials and have not been represented in other array collections. The primary screen was performed in 96-well plates. Wild-type, Megf10 shRNA and scrambled shRNA C2C12 myoblasts were seeded at a density of 1000 cells per well, calculated using a Countess Cell Counter. After a wait of 4 h to allow cells to adhere, drug compounds were administered in triplicate at 1 µM concentrations. Accounting for scrambled shRNA and wild-type C2C12 myoblast controls, as well as no drug treatment DMSO (0.1%) controls, all in triplicate, 27 compounds were tested on a typical 96-well plate. As cell proliferation was previously found to be significantly impaired in Megf10 deficiency (10), CyQuant assays were used 24 h after drug treatment to quantify cellular proliferation of each well. Data collected from the initial screen was analyzed using one-way ANOVA and *t*-test, the latter was conducted via comparisons with the DMSO vehicle controls. Any compounds that showed significant changes ($P < 0.05$) on either analysis were selected for repeat screening. Those compounds were not revealed to the experimenter until retested for the second time. Compounds that yielded augmented proliferation on both screens were then identified and selected for a dose response experiment that tested the selected drugs at 10, 1 and 0.1 µM concentrations.

Drugs for further analysis

The positive hits were confirmed by repeated independent cell proliferation assays on Megf10 shRNA C2C12 cells. On the initial screen, citalopram hydrobromide was identified as a modest hit. Further analyses were performed on escitalopram, which has been reported to be a more robust enantiomer of citalopram (43). HPLC-grade sertraline hydrochloride, escitalopram, losartan potassium, tolteradine L-tartrate and D-(+)-vesamicol hydrochloride were purchased (Sigma Aldrich) for further testing in secondary screens. These were administered at the same 1 µM concentration as in the primary screen for the second *in vitro* analyses.

Immortalized myoblast models generated by overexpression of mutant C774R MEGF10

V5-tagged human p.C774R mutant *MEGF10* (9) was also transfected into C2C12 cells, which were subsequently analyzed by fluorescence-activated cell sorting (FACS) (10).

Primary mouse myoblasts

Under an Institutional Animal Care and Use Committee (IACUC)-approved protocol at the University of Florida, myoblasts were isolated from the hind limb muscles of neonatal wild-type and Megf10$^{-/-}$ mice (the latter were kindly provided by Jeremy Kay and Joshua Sanes) (32) using a skeletal muscle dissociation kit (Miltenyi Biotech) and cultured in Ham's F10 nutrient medium (Life Technologies) with 20% fetal bovine serum (Sigma), penicillin (50 units/mL), streptomycin (50 µg/mL) and fibroblast growth factor (Promega) (10).

Human subject recruitment and reprogramming of mononuclear blood cells into iPSCs

Under an Institutional Review Board (IRB)-approved protocol at the University of Florida, blood samples were collected from five individuals affected by MEGF10 myopathy: 02-1, 03-1, 27-1, 27-3, 27-4 representing three families (Table 1), along with asymptomatic carriers 02-2 and 02-3 and a control subject (H). Peripheral blood mononuclear cells from these subjects were reprogrammed into iPSCs by transduction of the Sendai viral vector SeVdp(KOSM)302L encoding four reprogramming factors (Oct4, Sox2, Klf4 and c-Myc) (44). The iPSC culture medium consisted of mTeSR1 Basal Medium and mTeSR1 5X Supplement (STEMCELL Technologies). The genotypes of the cell lines used in this study were confirmed using standard Sanger sequencing techniques. Clinical information and clinical genetic test information was also obtained from the three families with their consent under the IRB protocol.

Differentiation of iPSCs into myoblasts followed by sertraline treatment

The protocol for differentiation of iPSCs into myogenic progenitor cells was modified from one described recently (45).

iPSC colonies cultured in 24-well plates were treated for 1 day with 10ng/mL FGF and 10 μM Y276369, 3 days with 3.0 μM CHIR99021 (Axon Medchem) and 9 days with 10 μM DAPT in myogenic differentiation medium (DMEM/F12; Gibco, N-2 supplement). DAPT was removed and cells were cultured in Skeletal Muscle Growth Medium (Promocell) containing Growth Supplement Mix, 20% FBS, GlutaMAX and Antibiotic-Antimycotic. Myoblasts were then cultured for an additional 7 days in Skeletal Muscle Differentiation Medium (Promocell) containing Differentiation Supplement Mix, 2% horse serum, GlutaMAX and Antibiotic-Antimycotic. Medium was refreshed daily. The iPSC-derived myoblasts were seeded on Matrigel-coated 96-well plates for drug treatment. Twenty-four hours after seeding, serum was retracted for 16 h. Sertraline was diluted in serum media and added to cells for a final concentration of 1 μM after 24 h of drug treatment, proliferation and migration.

RNA analysis

Total RNA was extracted from iPSC-derived human myoblasts using the RNAqueous-4PCR kit (Ambion, Thermo Fisher Scientific) and reverse transcribed to cDNA using the high-capacity RNA to cDNA kit (Applied Biosystems). RT-PCR of cDNA was performed using the TaqMan Gene Expression Master Mix and TaqMan primer probe set designed for *MEGF10*, *NOTCH1*, *HEY1*, *PAX7*, *ITGA7*, *MYOD*, *DMD*, *MHC7*, *TITIN*, *MYOG* with ribosomal RNA *18S* probe sets serving as controls (Thermo Fisher Scientific). Transcript levels were normalized to *18S* transcript levels using the ΔΔCT method (10).

Protein analysis

Protein was extracted from C2C12 cells by lysing the myoblasts in RIPA buffer (25 mM Tris-HCl pH 7.6, 150 mM NaCl, 1% NP-40, 1% sodium deoxycholate, 0.1% SDS, 1 mM phenylmethylsulfonyl fluoride, 50 mM NaF, 1 mM Na3VO4). Cell lysate was spun at 14 000*g* at 4°C for 20 min. The total protein content of the supernatant was measured (BCA, Sigma), and 50 μg of the extract was resolved on a 4–12% SDS-polyacrylamide gel (Life Technologies), then transferred onto a nitrocellulose membrane (20 μm). The membrane was blocked in 5% milk/TBST (0.5% Tween-20, 8 mM Tris-Base, 25 mM Tris-HCL, 154 mM NaCl), then probed with antibodies to Notch1 at a 1:500 dilution (DHSB) and Gapdh at a 1:1000 dilution (Cell Signaling Technologies). The membrane was incubated with horseradish peroxidase-conjugated secondary antibodies and visualized by chemiluminescence (Thermo Scientific).

Cell functional assays

Cell proliferation, adhesion and migration assays were performed and analyzed as previously described (10) on C2C12 myoblasts, primary mouse myoblasts and iPSC-derived human myoblasts. The CyQUANT Direct Cell Proliferation assay kit (Thermo Fisher Scientific) was used to assess cell proliferation. Cell adhesion assays were performed with the Vybranto Cell Adhesion Assay Kit (Life Technologies); calcein was added 24 h after drug treatment, followed by quantification of adherent cells at 30 and 60 min time points. A scratch migration assay was performed to assess cell migration. The plates were scratched using a 200 μL pipette tip 24 h after drug treatment to create cell free zones, with photographs taken at 24 and 72 h time points. Quantification of the migration results was performed using ImageJ (46).

Notch inhibition and serotonin pathway activation

For pathway manipulations, 2000 Megf10 shRNA and 1500 control shRNA treated C2C12 myoblasts were seeded and cultured for 24 h in a 96-well tissue culture plate. Serum was retracted from these cells for 16–18 h. The Notch inhibitor DAPT (Sigma) was added at 10 μM in the serum free media for an hour. Serotonin (Sigma) was diluted in 100% methanol and added at 40 μM in the serum free media for an hour. Pathway control wells received neither DAPT nor serotonin. After a quick wash with PBS, media with serum was added back to the wells along with 1 μM sertraline hydrochloride. Control wells received media without sertraline. After 24 h, cell proliferation was assessed as described above.

Assessment of sertraline treatment on the Notch pathway in human myoblasts

Total RNA was extracted from sertraline-treated and untreated human primary myoblast cell lines using the Purelink RNA extraction kit (Thermo Fisher Scientific). The RNA was reverse-transcribed to cDNA using a High-Capacity RNA-to-cDNA kit (Thermo Fisher Scientific). RT-PCR was performed with the TaqMan® Array, Human Notch Signaling, Fast 96-Well Plate (Thermofisher Scientific) to assess effects of sertraline treatment on the Notch pathway. Each plate contains 43 assays for Notch signaling associated genes and 5 assays for endogenous control genes (*18S*, *GAPDH*, *HPRT*, *GUSB*, *ACTB*), in duplicate. Each plate was used to compare sertraline treatment versus no treatment on myoblast lines representing MEGF10 myopathy patients (02-1, 03-1, 27-1) and a healthy control human cell line.

Drosophila studies

The $drpr^{\Delta 5}$ mutant fly line (genotype: w^-; *sp/CyO*; *drprΔ/TM6*, *sb*, *Tb*, *e*; where w^-; *sp/CyO*; *drprΔ5*/drprΔ5 null are adult viable) (12) was generously provided by Marc Freeman (Vollum Institute, Oregon Health Sciences University, Portland, OR, USA). The stock was maintained at 25°C in a 12 h light/12 h dark cycle on standard *Drosophila* media. Drug treatment was performed on two different genotypes in parallel (i) $drpr^{\Delta 5}$ heterozygous mutants (genotype: w^-; $sp/CyO^{act::GFP}$; $drprΔ5^{rec8\ (9)}$/*TM6*, *sb*, *Tb*, *e*) and (ii) $drpr^{\Delta 5}$ homozygous mutants (i.e. 'nulls', genotype: w^-; $sp/CyO^{act::GFP}$; $drprΔ5^{rec8\ (9)}/drprΔ5^{rec8\ (9)}$). The drug was delivered systemically to 1 day old adult flies (males or virgin females) at a 10^{-4}M concentration, in 0.1% DMSO/10% sucrose (vehicle control is 0.1% DMSO/10% sucrose). The flies fed directly on cotton swabs that were inserted into the vial and saturated daily with fresh solutions (+/− drug). The vials were maintained horizontally insuring easy access of the mutant flies to the food and placed in a humidified chamber. Of note, control flies can be readily maintained for more than 20 days on sucrose solution in this setup. Rescue of the shortened lifespan displayed by $drpr^{\Delta 5}$ null mutants (versus that of $drpr^{\Delta 5}$ heterozygote siblings) was used as a readout of drug effect. Independent groups of 9–14 flies per genotype (i.e. isolated at different generation times) were tested. In addition, flies bearing the $drpr^{\Delta 5}$ mutation in two different genetic backgrounds (i.e. in the original $white^-$ (w^-) isogenic background 1 (12), as well as in the wild-type w^+

background 2, in which the *drpr* mutation was backcrossed) were utilized.

Zebrafish studies

All zebrafish were housed in the Zebrafish Research Facility of the University of Alabama at Birmingham under animal protocol number IACUC-20320. AB strain zebrafish were used for all injections and served as wild-type controls when applicable. Megf10 mutant zebrafish (megf10^{sa13029}) contain a T to A nonsense mutation in exon 5 of zebrafish megf10 and were obtained from the Zebrafish International Resource Center (Eugene, OR) as fertilized embryos. The zebrafish megf10 mutation was detected using the following genotyping primers zmegf10_fwd: 5′ GATTATCTGATGTTTGAGGTACACTTATAGAGC 3′ and zmegf10_rev: 5′ CAGCTGCAGAACTTACCGCTGGAG 3′ via JumpStart Taq DNA Polymerase (Sigma) following the manufacturer's protocol and using standard PCR conditions. Heterozygote carriers of the mutation were identified via standard Sanger sequencing. Zebrafish were housed in either 1.8 or 3 l tanks, given shrimp feed and maintained under a 14:10 h light:dark cycle. Zebrafish were euthanized via immersion in tricaine methane sulfonate (MS222, 200 mg/l final concentration; Sigma-Aldrich; St. Louis, MO) consistent with ethically acceptable practices (47). Each individual drug was tested in duplicate, containing 25 embryos each (n = 50 total embryos per drug). Individual drugs were administered in the tanks at 2 dpf with final concentrations of 0.1 and 1 μM, as dissolved in 0.01% DMSO/fish water (vehicle control). As in primary screening, at 5 dpf, fish were assessed for abnormal skeletal muscle development via birefringence assay, dorsal muscle structure and overall viability. Drug compounds that had shown no phenotypic malformations of affected fish were categorized as 'corrected' mutants following confirmation of *megf10* mutation. All fish pools were screened for predicted Mendelian ratios of 25% wild type, 50% heterozygotes, and 25% mutants via heterozygote crossings.

Supplementary Material

Supplementary Material is available at *HMG* online.

Acknowledgements

The authors are grateful to the families who have enrolled in this study for their participation. The authors thank Jeremy Kay and Joshua Sanes for sharing the *Megf10*$^{-/-}$ mouse model and Marc Freeman for sharing the *drpr*$^{\Delta 5}$ mutant fly line.

Conflict of Interest statement. Medosome Biotec is working to develop this therapeutic approach further.

Funding

National Institutes of Health (R41AR068158); Ferlita Family Fund.

References

1. Hartley, L., Kinali, M., Knight, R., Mercuri, E., Hubner, C., Bertini, E., Manzur, A.Y., Jimenez-Mallebrera, C., Sewry, C.A. and Muntoni, F. (2007) A congenital myopathy with diaphragmatic weakness not linked to the SMARD1 locus. *Neuromuscul. Disord.*, **17**, 174–179.
2. Boyden, S.E., Mahoney, L.J., Kawahara, G., Myers, J.A., Mitsuhashi, S., Estrella, E.A., Duncan, A.R., Dey, F., DeChene, E.T., Blasko-Goehringer, J.M. *et al.* (2012) Mutations in the satellite cell gene MEGF10 cause a recessive congenital myopathy with minicores. *Neurogenetics*, **13**, 115–124.
3. Logan, C.V., Lucke, B., Pottinger, C., Abdelhamed, Z.A., Parry, D.A., Szymanska, K., Diggle, C.P., van Riesen, A., Morgan, J.E., Markham, G. *et al.* (2011) Mutations in MEGF10, a regulator of satellite cell myogenesis, cause early onset myopathy, areflexia, respiratory distress and dysphagia (EMARDD). *Nat. Genet.*, **43**, 1189–1192.
4. Pierson, T.M., Markello, T., Accardi, J., Wolfe, L., Adams, D., Sincan, M., Tarazi, N.M., Fajardo, K.F., Cherukuri, P.F., Bajraktari, I. *et al.* (2013) Novel SNP array analysis and exome sequencing detect a homozygous exon 7 deletion of MEGF10 causing early onset myopathy, areflexia, respiratory distress and dysphagia (EMARDD). *Neuromuscul. Disord.*, **23**, 483–488.
5. Holterman, C.E., Le Grand, F., Kuang, S., Seale, P. and Rudnicki, M.A. (2007) Megf10 regulates the progression of the satellite cell myogenic program. *J. Cell Biol.*, **179**, 911–922.
6. Liewluck, T., Milone, M., Tian, X., Engel, A.G., Staff, N.P. and Wong, L.J. (2016) Adult-onset respiratory insufficiency, scoliosis, and distal joint hyperlaxity in patients with multiminicore disease due to novel Megf10 mutations. *Muscle Nerve*, **53**, 984–988.
7. Takayama, K., Mitsuhashi, S., Shin, J.Y., Tanaka, R., Fujii, T., Tsuburaya, R., Mukaida, S., Noguchi, S., Nonaka, I. and Nishino, I. (2016) Japanese multiple epidermal growth factor 10 (MEGF10) myopathy with novel mutations: a phenotype-genotype correlation. *Neuromuscul. Disord.*, **26**, 604–609.
8. Suzuki, E. and Nakayama, M. (2007) The mammalian Ced-1 ortholog MEGF10/KIAA1780 displays a novel adhesion pattern. *Exp. Cell Res.*, **313**, 2451–2464.
9. Mitsuhashi, S., Mitsuhashi, H., Alexander, M.S., Sugimoto, H. and Kang, P.B. (2013) Cysteine mutations cause defective tyrosine phosphorylation in MEGF10 myopathy. *FEBS Lett.*, **587**, 2952–2957.
10. Saha, M., Mitsuhashi, S., Jones, M.D., Manko, K., Reddy, H.M., Bruels, C.C., Cho, K.A., Pacak, C.A., Draper, I. and Kang, P.B. (2017) Consequences of MEGF10 deficiency on myoblast function and Notch1 interactions. *Hum. Mol. Genet.*, **26**, 2984–3000.
11. Draper, I., Mahoney, L.J., Mitsuhashi, S., Pacak, C.A., Salomon, R.N. and Kang, P.B. (2014) Silencing of drpr leads to muscle and brain degeneration in adult Drosophila. *Am. J. Pathol.*, **184**, 2653–2661.
12. Freeman, M.R., Delrow, J., Kim, J., Johnson, E. and Doe, C.Q. (2003) Unwrapping glial biology: Gcm target genes regulating glial development, diversification, and function. *Neuron*, **38**, 567–580.
13. Haskell, G.T., Adams, M.C., Fan, Z., Amin, K., Guzman Badillo, R.J., Zhou, L., Bizon, C., Chahin, N., Greenwood, R.S., Milko, L.V. *et al.* (2018) Diagnostic utility of exome sequencing in the evaluation of neuromuscular disorders. *Neurol. Genet.*, **4**, e212.
14. Kang, H.L., Benzer, S. and Min, K.T. (2002) Life extension in drosophila by feeding a drug. *Proc. Natl. Acad. Sci. U. S. A.*, **99**, 838–843.
15. Wang, C., Wheeler, C.T., Alberico, T., Sun, X., Seeberger, J., Laslo, M., Spangler, E., Kern, B., de Cabo, R. and Zou, S. (2013) The effect of resveratrol on lifespan depends on both gender and dietary nutrient composition in Drosophila melanogaster. *Age (Dordr.)*, **35**, 69–81.

16. Chisari, C., Licitra, R., Pellegrini, M., Pellegrino, M. and Rossi, B. (2009) Fluoxetine blocks myotonic runs and reverts abnormal surface electromyogram pattern in patients with myotonic dystrophy type 1. *Clin. Neuropharmacol.*, **32**, 330–334.
17. Waugh, T.A., Horstick, E., Hur, J., Jackson, S.W., Davidson, A.E., Li, X. and Dowling, J.J. (2014) Fluoxetine prevents dystrophic changes in a zebrafish model of Duchenne muscular dystrophy. *Hum. Mol. Genet.*, **23**, 4651–4662.
18. Johnson, R.D., Lewis, R.J. and Angier, M.K. (2007) The distribution of fluoxetine in human fluids and tissues. *J. Anal. Toxicol.*, **31**, 409–414.
19. Luo, D., Renault, V.M. and Rando, T.A. (2005) The regulation of notch signaling in muscle stem cell activation and postnatal myogenesis. *Semin. Cell Dev. Biol.*, **16**, 612–622.
20. Pinchot, S.N., Jaskula-Sztul, R., Ning, L., Peters, N.R., Cook, M.R., Kunnimalaiyaan, M. and Chen, H. (2011) Identification and validation of notch pathway activating compounds through a novel high-throughput screening method. *Cancer*, **117**, 1386–1398.
21. Cray, J.J. Jr., Weinberg, S.M., Parsons, T.E., Howie, R.N., Elsalanty, M. and Yu, J.C. (2014) Selective serotonin reuptake inhibitor exposure alters osteoblast gene expression and craniofacial development in mice. *Birth Defects Res. A Clin. Mol. Teratol.*, **100**, 912–923.
22. Chen, H.F., Pan, X.L., Wang, J.W., Kong, H.M. and Fu, Y.M. (2014) Protein-drug interactome analysis of SSRI-mediated neurorecovery following stroke. *Biosystems*, **120**, 1–9.
23. Sui, Y., Zhang, Z., Guo, Y., Sun, Y., Zhang, X., Xie, C., Li, Y. and Xi, G. (2009) The function of Notch1 signaling was increased in parallel with neurogenesis in rat hippocampus after chronic fluoxetine administration. *Biol. Pharm. Bull.*, **32**, 1776–1782.
24. Ghareghani, M., Zibara, K., Sadeghi, H., Dokoohaki, S., Sadeghi, H., Aryanpour, R. and Ghanbari, A. (2017) Fluvoxamine stimulates oligodendrogenesis of cultured neural stem cells and attenuates inflammation and demyelination in an animal model of multiple sclerosis. *Sci. Rep.*, **7**, 4923.
25. Kim, H.S., Li, H., Kim, H.W., Shin, S.E., Choi, I.W., Firth, A.L., Bang, H., Bae, Y.M. and Park, W.S. (2016) Selective serotonin reuptake inhibitor sertraline inhibits voltage-dependent K+ channels in rabbit coronary arterial smooth muscle cells. *J. Biosci.*, **41**, 659–666.
26. Kim, H.S., Li, H., Kim, H.W., Shin, S.E., Seo, M.S., An, J.R., Ha, K.S., Han, E.T., Hong, S.H., Choi, I.W. *et al.* (2017) Escitalopram, a selective serotonin reuptake inhibitor, inhibits voltage-dependent K(+) channels in coronary arterial smooth muscle cells. *Korean J. Physiol. Pharmacol.*, **21**, 415–421.
27. Maciag, D., Simpson, K.L., Coppinger, D., Lu, Y., Wang, Y., Lin, R.C. and Paul, I.A. (2006) Neonatal antidepressant exposure has lasting effects on behavior and serotonin circuitry. *Neuropsychopharmacology*, **31**, 47–57.
28. Haskell, S.E., Hermann, G.M., Reinking, B.E., Volk, K.A., Peotta, V.A., Zhu, V. and Roghair, R.D. (2013) Sertraline exposure leads to small left heart syndrome in adult mice. *Pediatr. Res.*, **73**, 286–293.
29. Lugo-Candelas, C., Cha, J., Hong, S., Bastidas, V., Weissman, M., Fifer, W.P., Myers, M., Talati, A., Bansal, R., Peterson, B.S. *et al.* (2018) Associations between brain structure and connectivity in infants and exposure to selective serotonin reuptake inhibitors during pregnancy. *JAMA Pediatr.*, **172**, 525–533.
30. Zimmerman, A., Clemens, P.R., Tesi-Rocha, C., Connolly, A., Iannaccone, S.T., Kuntz, N., Arrieta, A., Hache, L., Henricson, E., Hu, F. *et al.* (2011) Liquid formulation of pentoxifylline is a poorly tolerated treatment for duchenne dystrophy. *Muscle Nerve*, **44**, 170–173.
31. Escolar, D.M., Zimmerman, A., Bertorini, T., Clemens, P.R., Connolly, A.M., Mesa, L., Gorni, K., Kornberg, A., Kolski, H., Kuntz, N. *et al.* (2012) Pentoxifylline as a rescue treatment for DMD: a randomized double-blind clinical trial. *Neurology*, **78**, 904–913.
32. Kay, J.N., Chu, M.W. and Sanes, J.R. (2012) MEGF10 and MEGF11 mediate homotypic interactions required for mosaic spacing of retinal neurons. *Nature*, **483**, 465–469.
33. Takahashi, K., Tanabe, K., Ohnuki, M., Narita, M., Ichisaka, T., Tomoda, K. and Yamanaka, S. (2007) Induction of pluripotent stem cells from adult human fibroblasts by defined factors. *Cell*, **131**, 861–872.
34. Yu, J., Vodyanik, M.A., Smuga-Otto, K., Antosiewicz-Bourget, J., Frane, J.L., Tian, S., Nie, J., Jonsdottir, G.A., Ruotti, V., Stewart, R. *et al.* (2007) Induced pluripotent stem cell lines derived from human somatic cells. *Science*, **318**, 1917–1920.
35. Robinton, D.A. and Daley, G.Q. (2012) The promise of induced pluripotent stem cells in research and therapy. *Nature*, **481**, 295–305.
36. Hankowski, K.E., Hamazaki, T., Umezawa, A. and Terada, N. (2011) Induced pluripotent stem cells as a next-generation biomedical interface. *Lab. Invest.*, **91**, 972–977.
37. Ebert, A.D., Yu, J., Rose, F.F. Jr., Mattis, V.B., Lorson, C.L., Thomson, J.A. and Svendsen, C.N. (2009) Induced pluripotent stem cells from a spinal muscular atrophy patient. *Nature*, **457**, 277–280.
38. Itzhaki, I., Maizels, L., Huber, I., Zwi-Dantsis, L., Caspi, O., Winterstern, A., Feldman, O., Gepstein, A., Arbel, G., Hammerman, H. *et al.* (2011) Modelling the long QT syndrome with induced pluripotent stem cells. *Nature*, **471**, 225–229.
39. Berger, J. and Currie, P.D. (2012) Zebrafish models flex their muscles to shed light on muscular dystrophies. *Dis. Model Mech.*, **5**, 726–732.
40. Strange, K. (2016) Drug discovery in fish, flies, and worms. *ILAR J.*, **57**, 133–143.
41. Draper, I. (2013) Model organisms offer new possibilities for discovery of therapeutics. *Drug Discov. Today Technol.*, **10**, e61–e64.
42. Kreipke, R.E., Kwon, Y.V., Shcherbata, H.R. and Ruohola-Baker, H. (2017) Drosophila melanogaster as a model of muscle degeneration disorders. *Curr. Top. Dev. Biol.*, **121**, 83–109.
43. Montgomery, S., Hansen, T. and Kasper, S. (2011) Efficacy of escitalopram compared to citalopram: a meta-analysis. *Int. J. Neuropsychopharmacol.*, **14**, 261–268.
44. Santostefano, K.E., Hamazaki, T., Biel, N.M., Jin, S., Umezawa, A. and Terada, N. (2015) A practical guide to induced pluripotent stem cell research using patient samples. *Lab. Invest.*, **95**, 4–13.
45. Choi, I.Y., Lim, H., Estrellas, K., Mula, J., Cohen, T.V., Zhang, Y., Donnelly, C.J., Richard, J.-P., Kim, Y.J., Kim, H. *et al.* (2016) Concordant but varied phenotypes among Duchenne muscular dystrophy patient-specific myoblasts derived using a human iPSC-based model. *Cell Rep.*, **15**, 2301–2312.
46. Chakraborty, S., Lakshmanan, M., Swa, H.L., Chen, J., Zhang, X., Ong, Y.S., Loo, L.S., Akincilar, S.C., Gunaratne, J., Tergaonkar, V. *et al.* (2015) An oncogenic role of Agrin in regulating focal adhesion integrity in hepatocellular carcinoma. *Nat. Commun.*, **6**, 6184.
47. Strykowski, J.L. and Schech, J.M. (2015) Effectiveness of recommended euthanasia methods in larval zebrafish (Danio rerio). *J. Am. Assoc. Lab. Anim. Sci.*, **54**, 76–79.